Editor Recommendation: Original Article

Current Urology

OPEN

In vivo photobleaching kinetics and epithelial biodistribution of hexylaminolevulinate-induced protoporphyrin IX in rat bladder cancer

Sami El Khatib*

Department of Biological Sciences, Lebanese International University, Bekaa Campus, Khiyara, Lebanon

Abstract

In a previous paper, we showed that rat bladder instillations with 8 or 16 mM of hexyl aminolevulinate (hALA) result in diametrically opposed photodynamic therapy efficiency. Although the same fluorescent intensities were detected spectroscopically and by fluorescent microscopy in both conditions, while a given light dose resulted in tumor necrosis with an intact bladder wall after 8 mM hALA, bladders instilled with 16 mM showed total wall necrosis without impact on the tumor. The current study investigated the photobleaching and localization pattern of protoporphyrin IX (PpIX) after both hALA intravesical instillations in tumor-bearing rat bladders. The total PpIX content was evaluated by the extraction of postmortem whole bladders. Photobleaching was evaluated in vivo by fluorescent spectroscopy. Cryosections of bladders were subjected to fluorescent microscopy for cellular localization of the photosensitizer. PpIX extraction showed identical amounts of photosensitizer in tumor-bearing bladders at both concentrations. Photobleaching experiments revealed mono-exponential decay curves in both situations but with a two times faster decay constant in 16 mM bladders. Fluorescent microscopy showed an identical fluorescent pattern for normal bladders at both concentrations and tumor bladders at 8 mM with bright spots. Tumor bladders at 16 mM exhibited a more diffuse cytoplasmatic fluorescent distribution. The different response to photodynamic therapy with regard to the initial pro-drug concentration can thus be attributed to the different cellular localizations.

Keywords: Bladder cancer; Bladder carcinoma; Photodiagnosis; Photodynamic therapy; Urothelial carcinoma

1. Introduction

Photodynamic therapy (PDT) is a treatment modality based on the cytotoxic effect occurring in the target tissues by the interaction of a photosensitizer with light in the presence of oxygen.[1] One of the major advances in PDT is due to the use of topical aminolevulinate (ALA) to induce protoporphyrin IX (PpIX) for the treatment of early-stage cancers as well as in diagnosis.[2] ALA is a precursor of the heme synthesis pathway. Locally delivered to the target tissue, ALA overcomes the negative feedback exerted by heme and promotes the transient formation of PpIX in situ to reach critical effective levels in cells and tissues.[3] Although early steps of the heme pathway occur in the cytosol, PpIX synthesis is in the mitochondrial membranes[4] and PpIX fluorescence accumulates in close vicinity of the initial building site and progressively diffuses to the neighboring cytoplasmic compartment or other lipophylic organelles.[3,5,6]

PpIX is highly reactive and will degrade when irradiated with light. PpIX photobleaching is governed by a singlet oxygen-mediated mechanism in the presence of oxidized amino acids and proteins.[7] PpIX photobleaching and subsequent spectral photo-transformation were described in tumor cells incubated in vitro with ALA solution,[8] or ex vivo in human and porcine mucosa super-fused with hexyl aminolevulinate (hALA).[9] PpIX photo-bleaching was also studied in vivo, using animal models such as normal or tumor mouse skin[10,11] and the orthotopic rat bladder model.[3]

hALA, a more potent lipophilic derivative of ALA, was proposed as an adjunct to standard cystoscopy in the fluorescent diagnosis of bladder cancer[12,13] and other malignancies.[14,15] At the clinical level, hALA-induced fluorescent cystoscopy significantly improves detection of bladder cancer leading to a more complete resection and significantly better disease-free survival[16] with a trend towards improved bladder preservation.[17] The adoption of hALA photodiagnosis for bladder tumor resections in routine clinical practice is associated with reduced recurrence rates, in particularly in high-risk disease.[18] Importantly, hALA-mediated PDT does not induce evident macroscopic injury to normal cervical tissue 6 months after PDT. Microscopic analysis revealed no signs of apoptosis, necrosis, irritation, vascular changes, or fibroses.[19]

We previously reported the effectiveness of hALA-mediated PDT of rat bladder cancer.[20] Although normal and tumor bladder epithelium exhibit similar fluorescent intensities after intravesical instillation of 2 hALA concentrations (8 and 16 mM),

* *Corresponding Author: Sami El Khatib, Department of Biological Sciences, Lebanese International University, Bekaa Campus, LB–1108 Khiyara (Lebanon). E-mail address: sami.khatib@liu.edu.lb (S. El. Khatib).*

Current Urology, (2021) 15, 2-10

Received July 16, 2019; Accepted September 16, 2019.

http://dx.doi.org/10.1097/CU9.0000000000000004

the therapeutic response at 8 mM and 20 J/cm^2 were completely different from the one observed at 16 mM irradiated with the same light dose. Although the tumor is destroyed, leaving the underlying submucosa and muscle intact after an 8 mM instillation, 16 mM sensitization and subsequent illumination results in the complete destruction of the underlying bladder wall but leaves the tumor undamaged.

The objective of the current study is to try to unravel the underlying mechanism for this apparent contradiction.

2. Materials and methods

2.1. Bladder cancer cell line

The tumor cell line (AY27) was initially derived from carcinomas of the urinary bladder induced in female Fischer (F344) rats fed continuously with N-[4-(5-Nitro-2-furyl)-2-thiazolyl] formamide. The papillary transitional AY27 cell line was primarily established by subcutaneous transplantation and subsequently established in cell culture. The cell line was a generous gift to our laboratory by Drs S. Selman and J. Hampton from the Medical College of Ohio (Toledo, OH). The culture medium used was RPMI-1640 (GIBCO, Invitrogen, UK), supplemented with 5% L-glutamine (200 mM), 5% penicillin-streptomycin, and 10% fetal calf serum (Biotech, GmbH). Cells were cultured in 75 cm^2 tissue culture flasks with a 0.2 μm vented cap (BD Biosciences) and maintained in a humidified incubator with 5% CO_2. At confluence, cultured cells were dissociated with 10 ml Trypsin-EDTA for 10 minutes at 37°C and then centrifuged and re-suspended in complemented RPMI 1640 medium. Cell viability was determined by the standard trypan blue (0.4%) exclusion test.

2.2. Animal tumor model

Female Fischer (F344) rats weighting 160–200 g were purchased from Harlan Laboratories (France). Animals were maintained in our animal care facility and housed 4 per cage at room temperature (22 ± 2°C) with food and water ad libidum. The orthotopic bladder cancer model was previously described by Xiao et al.[21] Briefly, animals were anesthetized with an intraperitoneal injection of 45 mg/kg of sodium pentobarbital (Sanofi, France) and the body temperature was maintained with a thermostatic blanket during experiments. The rats' bladders were catheterized with a 16G intravenous cannula (Terumo, Surflo). Epithelial desquamation was performed using an intravesical instillation of 0.5 ml HCl (0.1 N) for 15 seconds, and neutralized with 0.5 ml of NaOH (0.1 N). Bladders were washed and a bladder tumor cell suspension (0.5 ml containing 10^6 cells) was intravesically instilled for 1 hour. Photobleaching experiments were carried out in normal and tumor-bearing rats 14 days after the implantation of tumor cells.

2.3. hALA administration

There were 2 hALA concentrations (8 and 16 mM) used in this study. The solutions were freshly prepared by dissolving hALA powder in phosphate-buffered saline (PBS). Animals were anesthetized and catheterized as previously described with a 14G intravenous cannula (Terumo, Surflo). 0.5 ml of hALA (8 and 16 mM) was intravesically administered in normal or tumor-bearing rat bladders for 1 hour, and the bladders were then emptied and washed with PBS. Light irradiation and fluorescent photobleaching measurements were performed 2 or 3 hours after the termination of the 8 or 16 mM instillation, respectively.

2.4. PpIX tissue extraction

PpIX was extracted according to a previous published method.[22] In brief, 2 and 3 hours after the end of a 1-hour intravesical instillation of hALA at 8 or 16 mM concentrations, the animals were euthanized and a cystectomy was performed. Healthy and tumor bladders of approximately 0.1–0.4 g wet weight were chopped into small pieces (approximately 0.05 g) using a scalpel, then immersed in 2 ml of Solvable™ in a 15 ml plastic tissue culture tube and placed into a water bath at 50°C for 1 h. The sample was then mechanically homogenized in the same vial and 5 aliquots of 0.2 ml of the resulting homogenate were diluted with 1 ml Solvable™ and 3 ml distilled water and returned to the water bath for a further 1 hour. If required, homogenate samples were diluted with distilled water to achieve an optical density < 0.1 and the fluorescence was measured in a 10 mm path length quartz cuvette using a Xenius spectrofluorimeter (SAFAS SA, Monaco). PpIX concentrations were then reported in μg/g of tissue by adding a volume of known PpIX concentration to the extracted sample.

2.5. Photodynamic treatment and photobleaching measurement

Fluorescent spectroscopy was performed using a CP-200 optical multichannel analyser (Jobin-Yvon) managed by Spectramax software (Molecular Devices, LLC). A bifurcated optical fiber was held in direct contact with the normal or tumor bladder. The first fiber was coupled to a diode laser (Type PPMT 25, 410 ± 5 nm) ensuring the excitation. The second fiber was coupled to the spectrofluorimeter with a charge-coupled device captor and transferred to a PC for fluorescent spectra acquisition. The fluorescent signal was collected through the wavelength bandwidth of 400–800 nm.

Whole bladder irradiation was performed using an argon pumped dye laser (Spectra Physics 2020, Les Ulis, France) coupled to an isotropic diffuser (IP159 Medlight S.A., Eccublens, Switzerland) placed in a central position in the bladder filled with 0.5 ml of PBS. The optical fiber and the diffuser were introduced into the bladder through a 2-port connector (Qosina, USA) screwed on a 14G catheter already introduced into the bladder. The initial fluorescent intensity was measured immediately before treatment, and 2 and 3 hours after the end of instillation of 8 and 16 mM hALA, respectively. During irradiation, the fluence rate was fixed at 100 mW/cm^2 and a total dose of 20 J/cm^2 was delivered into the bladder. The fluorescence was measured after the delivery of 1, 2, 4, 6, 8, 10, 12, 15, and 20 J/cm^2. In the case of tumor-bearing bladders a laparatomy was performed in order to target the tumor tissue during measurement with the help of light transmitted through the bladder wall.[20] A set of 4 normal rats and 5 tumor-bearing rats was used for each concentration of hALA (8, 16 mM) with a total of 18 rats included in the photobleaching study.

2.6. Data analysis

The fluorescent spectra were recorded in the wavelength bandwidth from 400 to 800 nm. Fluorescent areas were calculated by signal integration in the bandwidth between 620 and 650 nm and normalized according to the integrated autofluorescent area calculated in the bandwidth between 500 and 600 nm. For each animal, the values of fluorescence obtained during illumination were normalized to the initial fluorescent intensity in order to allow inter-animal comparisons. Photobleaching kinetics were separately fitted as a first-order decay using Sigmaplot® software and photobleaching decay constants were deduced from the fitted curves.

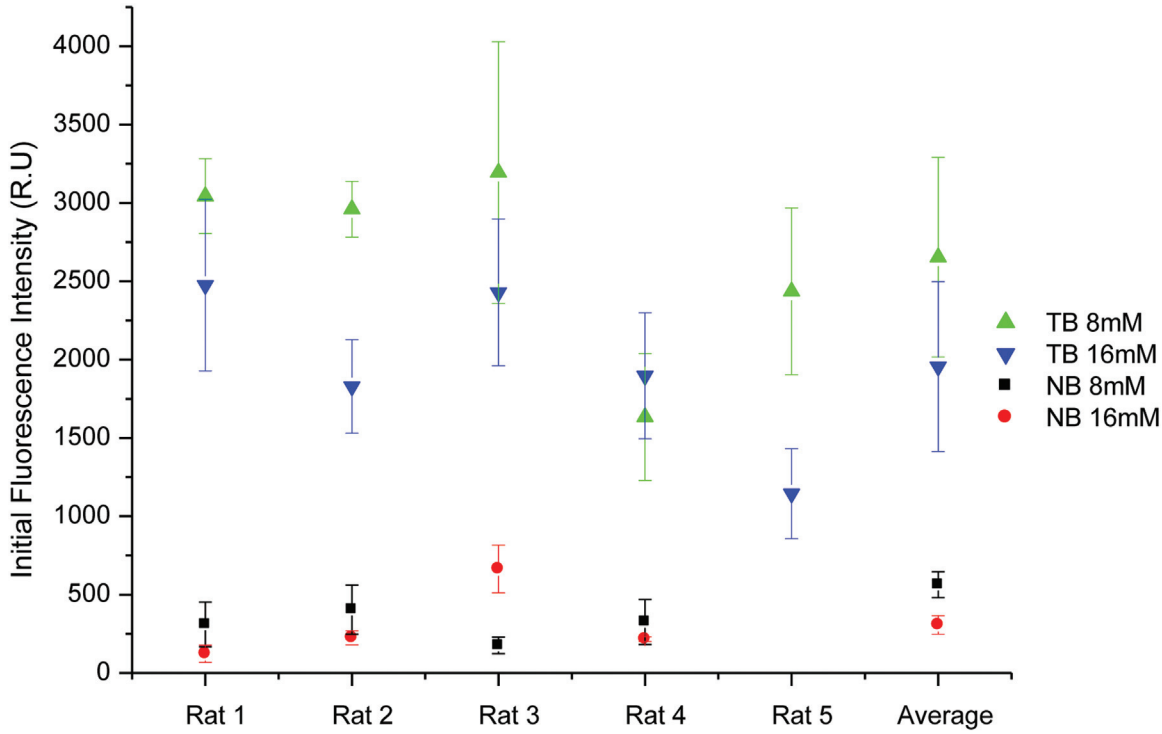

Figure 1. Initial fluorescent intensity obtained from normal (4 rats) and tumor (5 rats) rat bladders 2 and 3 hours after the end of intravesical instillation of 8 and 16 mM hALA (▲: Tumor bladder, 8 mM; ▼: tumor bladder, 16 mM; ■: normal bladder, 8 mM; ●: normal bladder, 16 mM).

2.7. Fluorescent confocal microscopy

Epithelial localization of hALA-induced PpIX was performed on cryosections using a fluorescent confocal (Nikon TE2000-U microscope linked with a Biorad LRC Radiance 2100 fitted with a 100 mW argon ion laser). Excitation was performed using a 514 nm diode laser and fluo, 166 line per second scan). After 2 and 3 hours after the end of hALA instillation of 8 and 16 mM, respectively, bladders were excised and embedded in tissue freezing medium (Tissue Tek) and kept at −80°C for 1 hour. Ten μm frozen sections were prepared and examined under a microscope using Sharp2000 software (Bio-Rad Laboratories, Inc).

Rescence was collected using a ×40 dic Nikon oil immersion objective with a lateral resolution of 0.15 μm and an axial resolution of 1.52 μm. PpIX fluorescence was collected using a HQ590LP filter collecting fluorescent signals above 590 nm. The final fluorescent images were constructed using a photocounting process (512 × 512 pixels, 302 × 302 μm, or 76 × 76 μm field of vision).

3. Results

3.1. Fluorescent intensity and PpIX content before treatment

Figure 1 shows the initial fluorescent intensities acquired in vivo from sensitized rat bladders 2 and 3 hours after the end of the hALA instillation of 8 or 16 mM hALA in healthy and tumor rat bladders immediately before treatment, respectively. The mean fluorescent intensities acquired by fluorescent spectroscopy at these endpoints are comparable for tumor bladders at both concentrations and are 4–6 fold higher than in normal bladders.

Figure 2 represents the PpIX content extracted ex vivo from healthy and tumor bladders 2 and 3 hours after the end of intravesical instillation of 8 and 16 mM hALA, respectively. At both concentrations, sensitized bladders accumulated a comparable porphyrin amount in normal as in tumor-bearing rat bladders with a tumor to normal ratio of 4.75 at 8 mM and 4.0 at 16 mM hALA.

3.2. Fluorescent spectroscopy during light irradiation

Figure 3 shows a set of mean fluorescent spectra acquired in vivo from a tumor-bearing rat bladder excited at 405 nm before and during irradiation with a total light dose of 20 J/cm^2 delivered at

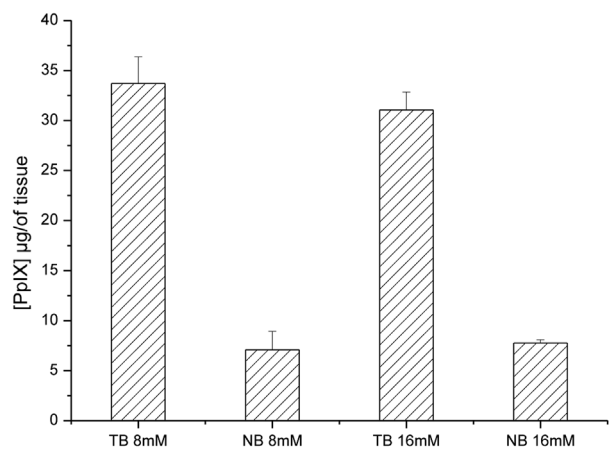

Figure 2. PpIX fluorescent concentrations extracted ex vivo from normal (NB) and tumor (TB) bladder tissues 2 and 3 hours after the end of intravesical instillation of 8 and 16 mM hALA, respectively.

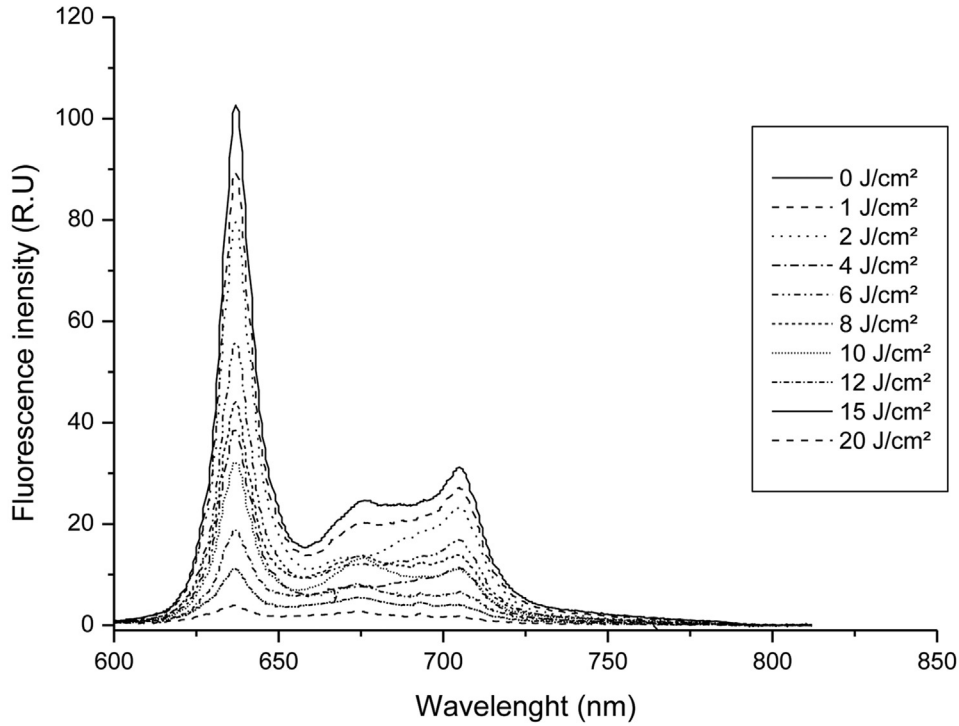

Figure 3. Set of mean fluorescent spectra acquired in vivo from a tumor-bearing rat bladder excited at 405 nm before (0 J/cm^2) and during irradiation (1–20 J/cm^2) with a total light dose of 20 J/cm^2 delivered at 630 nm with an incident fluence rate of 100 mW/cm^2.

630 nm with an incident fluence rate of 100 mW/cm^2. Irradiation was regularly interrupted to allow spectral measurements inside the bladders. The fluorescent emission spectrum exhibited a main fluorescent peak at 630 nm corresponding to PpIX fluorescence. The main spectral changes were attributed to the PpIX fluorescence decrease at 630 nm and the appearance of a novel fluorescent peak around 670 nm, which can be attributed to the photoproducts formation. Figure 4 shows the in vivo photobleaching kinetics from normal and tumor-bearing rat bladders. The PpIX fluorescence rapidly bleached and the fluorescence decrease was noted as early as the first delivered light dose (within 10 seconds of irradiation corresponding to 1 J/cm^2). Before plotting, initial fluorescent intensities were normalized to a standard value of 100 and photobleaching kinetics were plotted against the light doses delivered to a total fluence of 20 J/cm^2 and then monoexponentially fitted for all curves. In normal bladders PpIX fluorescent kinetics exponentially decreased with similar decay constants at 8 mM (0.2750 J/cm^2) and 16 mM (0.2781 J/cm^2). In tumor bladders sensitized with 8 mM, the PpIX fluorescence similarly bleached with a comparable (0.2621 J/cm^2). Only tumor bladders sensitized with 16 mM bleached more rapidly with a decay constant of 0.6268 J/cm^2.

3.3. Fluorescent confocal microscopy

Figure 5 shows images of the intracellular localization of PpIX 2 and 3 hours after the end of an intravesical instillation of 8 or 16 mM hALA. At 8 mM hALA, 2 hours after the end of instillation, healthy urothelium (Fig. 5A) and transitional cell carcinoma (Fig. 5C) show the presence of bright fluorescent spots. At 16 mM hALA, normal urothelium from healthy as well as from tumor-bearing bladders exhibited the same fluorescent distribution pattern (Fig. 5B). However, transformed AY27 epithelium exhibited a more diffuse cytoplasmic fluorescent distribution (Fig. 5D).

The whole image area plotted using Image J software (National Institutes of Health) shows that narrow-band emission peaks with comparable fluorescent intensities corresponding to the bright spots observed at 8 mM in healthy and tumor bladders and those observed at 16 mM in healthy bladders (Fig. 6A–C). However, a diffuse fluorescent distribution without distinct peaks was observed in tumor bladders cells at 16 mM (Fig. 6D).

Figure 7 shows confocal fluorescent images obtained from tumor rat bladders with either 8 mM (Fig. 7A) or 16 mM hALA (Fig. 7B). An 8 mM hALA instillation resulted in the same localization pattern for both normal and transformed urothelium. However, a 16 mM hALA instillation shows an identical punctuated distribution in normal urothelium, whereas the tumor has diffuse cytoplasmatic fluorescent localization.

4. Discussion

In a previous paper, we described the inverse effect obtained with bladder PDT under identical conditions except for the sensitizer concentrations.[20] Although perfect tumor destruction with an intact bladder wall was obtained with an 8 mM hALA instillation, 16 mM PDT under the same conditions (20 J/cm^2, 100 mW/cm^2) completely destroyed the bladder wall but left the tumor intact. The same fluorescent intensities were measured both in situ in vivo and on fluorescent microscopy ex vivo, but the fluorescence is not necessarily directly related to the concentration. Indeed, aggregates fluoresce less than monomers and have a reduced photodynamic activity.[23] We thus hypothesized that 16 mM hALA would induce a higher PpIX production in the tumor as well as in the underlying muscle but still results in monomeric

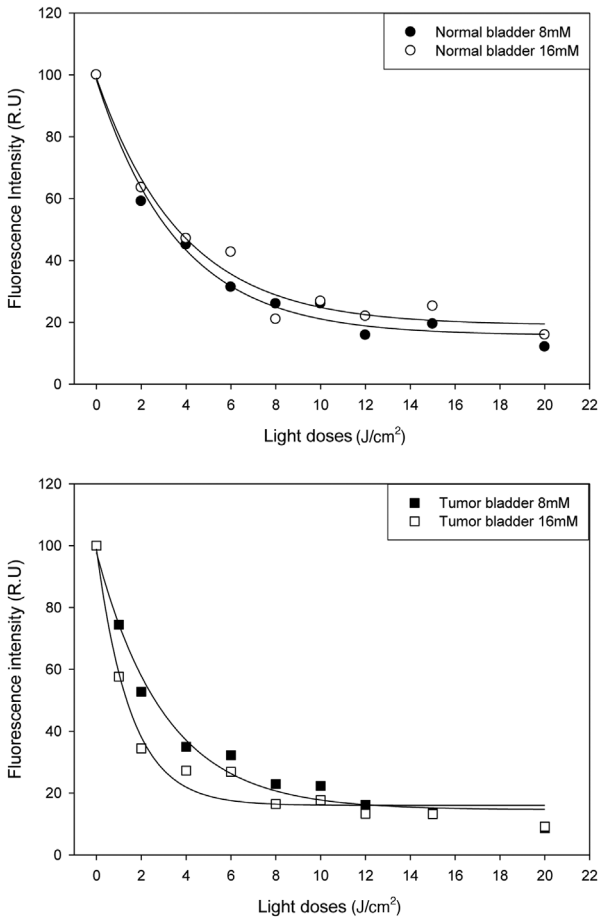

Figure 4. Photobleaching kinetics of PpIX in normal (top panel) and tumor rat bladders (bottom panel) during light irradiation with the same light conditions (fluence rate 100 mW/cm^2 and total fluence 20 J/cm^2). Bladders were sensitized with hALA and irradiated 2 and 3 hours after the end of intravesical instillation of 8 and 16 mM hALA, respectively.

PpIX in the latter, whereas PpIX would be more aggregated in the former.

From our extraction study, it appears that independent of the initial concentration of hALA, the PpIX content of the bladder is identical for 8 or 16 mM hALA instillation. However, the extraction procedure was performed on whole bladder tissue without separating the urothelial compartment from the rest of the bladder wall. Dissociation of the mucosa from the underlying submucosa and muscle can be obtained with certain procedures, but they have long incubation periods. Unfortunately, these techniques could not be applied in this study since it was shown in humans[24] and in animal studies[20] that PpIX is not retained within the epithelial cells after 3 hours. hALA being a pro-drug does not behave like most sensitizers, where increasing the drug dose will lead to enhanced uptake. It was shown for many cell lines including AY27, which PpIX builds up much faster after hALA incubation than with the nonesterified ALA, due to the passive diffusion of the ester rather than active transport for ALA.[25] But increasing the pro-drug concentration does not necessarily lead to increasing PpIX content of the AY27 cells.[26] This can either be attributed to esterase activity[23] being the rate limiting step[10] or the more efficient efflux of PpIX in transitional cell carcinoma.[3,26] Although extraction could not be performed on the epithelium without interference of the underlying muscle, previously mentioned data suggested that the epithelial concentration of PpIX is identical and independent of the initial hALA concentration.

To confirm this, we studied the photobleaching of PpIX in vivo. In general, as well as for PpIX, photobleaching is dependent on the aggregation state of the molecules.[23,27–29] Photobleaching of PpIX is a singlet oxygen-dependent process and the photobleaching rate of monomers is faster than that of aggregates due to the poor accessibility of O_2 within the core of the aggregate.[8] Although monomers exhibit a single exponential decay, a mixture of monomers and aggregates shows a bi- or pluri-exponential decay.[8,28] In these circumstances, the first fast part of the photobleaching curve can be attributed to the photobleaching of the monomers, whereas the second corresponds to the slower bleaching of the aggregates. Previous studies on PpIX photobleaching in vivo showed that the skin and esophageal photobleaching kinetics are nonexponential due to the bleaching of other nonphotosensitizer compounds within the cells.[11,30] All photobleaching curves in our study best fitted with a mono-exponential decay, including the tumors at 16 mM, thus pointing toward purely monomeric PpIX and rather tending to confirm identical concentrations of PpIX as suggested by previously mentioned fluorescent and extraction studies.

Although bleaching in the autofluorescent area was observed by 1 group in mouse skin,[31] this was not the case in human volunteers[32] nor did we observe any decrease in autofluorescence in rat bladders. As previously shown in solution, a complex mixture of photoproducts is formed after illumination of PpIX, the main being photoprotoporphyrin with a strong emission band around 675 nm.[33] Unlike the authors, we did not see any bleaching of the photoproduct in vivo, probably due to the lower excitation intensity used (20 J/cm^2) where bleaching of photoprotoporphyrin is only observed at fluences exceeding 30 J with comparable fluence rates as used in our study. Photobleaching constants of normal bladders at 8 and 16 mM as well as tumor bladders at 8 mM were identical (± 0.3 J/cm^2) and so was their clinical response to illumination. The photobleaching constant for tumors at 16 mM is singled out from these (0.6 J/cm^2), as is the PDT response (bladder wall necrosis, no tumoricidal effect). Since the photobleaching rate at 16 mM is two times faster, but still mono-exponential, this rules out the presence of aggregates, either pure or mixed with monomers.

In our study, the differences in the clinical behavior of tumors to PDT after 8 or 16 mM hALA instillation, could not be attributed to the concentration or aggregation state of PpIX. Nevertheless, photobleaching rates differed by a factor of 2, suggesting a possible different intracellular localization pattern, as another factor influencing photobleaching is the intracellular localization.[34] Photobleaching of porphyrins appears to be faster when located in the cytoplasm as opposed to cell organelles.[35] Others pointed out that re-localization could occur during illumination, which could explain the pluri-exponentiality of photobleaching decay curves.[8,36] Ex vivo fluorescent microscopy of the excised bladders demonstrated the presence of bright fluorescent spots in normal epithelium after 8 and 16 mM hALA instillations, as well as in transformed AY27 urothelium after 8 mM instillation. In contrast, tumors at 16 mM exhibited a diffuse cytoplasmatic fluorescent pattern. They also had a two times faster photobleaching constant, which correlates with the observations by Schneckenburger et al.[35]

Esterification of ALA does not interfere with the intracellular localization that remains mitochondrial as described either

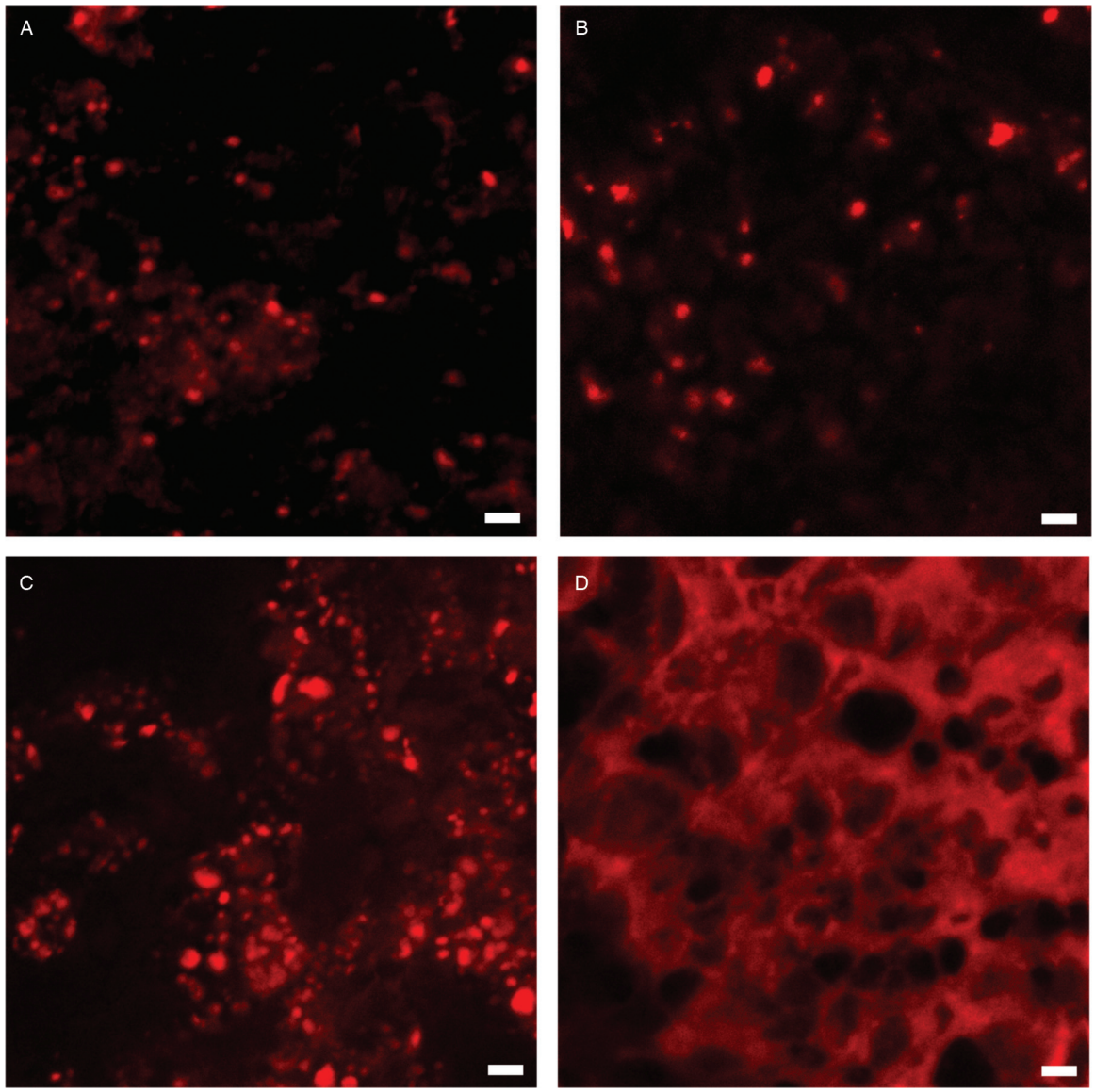

Figure 5. Fluorescent confocal microscopy of epithelial PpIX distribution obtained from normal (A, B) and tumor (C, D) rat bladders 2 and 3 hours after the end of intravesical instillation of 8 or 16 mM hALA, respectively. (A) normal bladder, 8 mM hALA, 1 + 2 hour. (B) normal bladder, 16 mM hALA, 1 + 3 hour. (C) tumor bladder, 8 mM hALA, 1 + 2 hour. (D) tumor bladder, 16 mM hALA, 1 + 3 hour. Scale bar = 5 μm, reduced from × 40 dic, Zoom × 4 (Field of view = 76 × 76 μm).

directly by fluorescent microscopy and mitochondria specific dyes, or indirectly through the detection of mitochondrial damage after illumination (electron microscopy, apoptosis, and mitochondrial activity).[37–39] We presume that the bright spots observed in normal urothelium at 8 and 16 mM and tumors at 8 mM can be attributed to this mitochondrial localization. In vivo instillation of the bladders with a mitochondrial marker (Mitotracker) in order to co-localize PpIX and mitochondria proved to be useless since there was a diffuse cytoplasmatic staining, as opposed to the selective fluorescent localization obtained in vitro (data not shown). We previously mentioned the possibility of using Rhodamine 123 intravesically in rats to stain epithelial and AY27 cells.[40] In this study, a concentration of 100 μM was used in order to stain the cell membrane. Concentrations below 25 μM, which are mitochondria specific in vitro, did not enhance specificity and the fluorescent distribution pattern remained diffuse (data not shown). Nevertheless, with regard to the fact that PpIX is synthesized in the mitochondria, that PpIX was shown in vitro to localize in the mitochondria, and the fact that the primary damage site of hALA-induced PDT was shown to be localized in the same organelles, we assume that the bright spots visualized in tissue that responds 'adequately' to PDT correspond to mitochondria. More precise subcellular localization (or exclusion thereof) could not be demonstrated because of the apparent lack of specificity of different markers after in vivo intravesical instillation.

Although the amount of intracellular photosensitizer is crucial for photodynamic efficacy, the intracellular localization is also very important.[41] According to the localization of PpIX (cell membrane, cytosol, or mitochondria), the response can vary from growth arrest, over apoptosis, to full necrosis.[42] The apparent resistance of some cell lines to PDT was shown to be correlated with diffuse cytoplasmatic localization of the photosensitizer (exogenous PpIX) as opposed to the mitochondrial localization

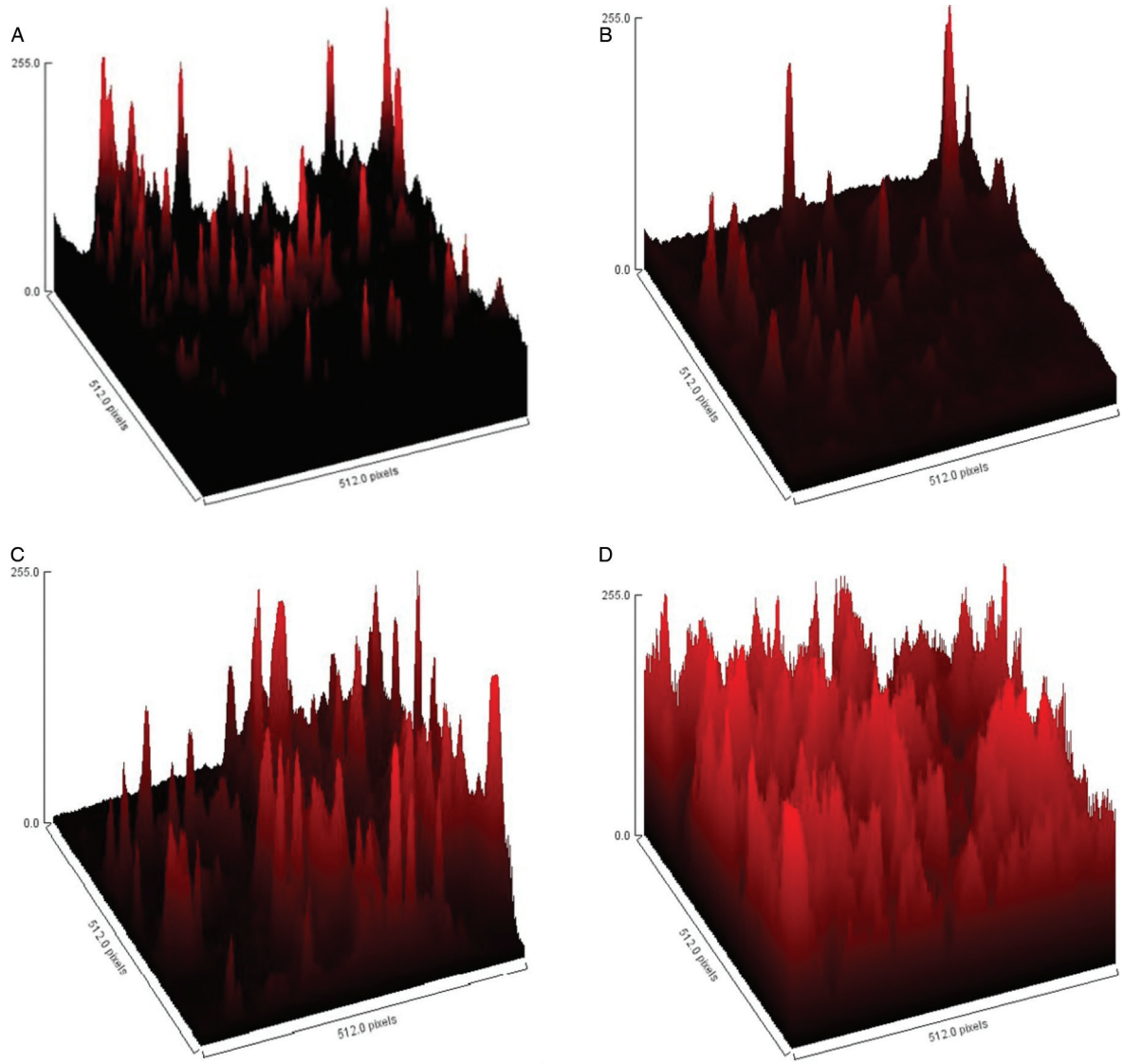

Figure 6. Fluorescent surface plot using Image J software obtained from normal (A, B) and tumor (C, D) rat bladders 2 and 3 hours after the end of intravesical instillation of 8 or 16 mM hALA, respectively. (A) normal bladder, 8 mM hALA, 1 + 2 hour. (B) normal bladder, 16 mM hALA, 1 + 3 hour. (C) tumor bladder, 8 mM hALA, 1 + 2 hour. (D) tumor bladder, 16 mM hALA, 1 + 3 hour. Surface plot = 76 × 76 μm.

of ALA-induced PpIX.[6] Regarding the incubation time of ALA, the PpIX localization within the cell starts as mitochondrial (where it is synthesized) and later becomes diffuse cytoplasmic. Accordingly, PDT efficacy is the highest at shorter incubation times and gradually decreases.[6] This same relocalization pattern was confirmed by Krammer and Uberriegler.[42] Our PDT experiments were performed after 1-hour incubation with the pro-drug, followed by a 2 or 3 hour resting time for 8 and 16 mM hALA, respectively. However, this 1-hour difference in incubation cannot explain the different localization of PpIX in tumors since adding 1 resting hour (to reach 1 + 3) in 8 mM tumor bladders or a 1-hour reduction to 2 hours (to reach 1 + 2) in case of 16 mM tumor, did not alter the specific localization with bright spots in case of 8 mM and diffuse cytoplasmic staining for 16 mM (data not shown). Worth mentioning is that Krammer and Uberriegler[42] demonstrated that low ALA incubation concentrations (100 μg/ml) produced a diffuse fluorescence, whereas a 10-fold increase (1 mg/ml) in ALA resulted in a more localized granular distribution pattern. No colocalization studies were performed, but the granules were presumed to be mitochondria where diffuse cytoplasmatic localization was suggested for the lower concentrations. No conclusions could be drawn from this study, although the authors suggested the granular localization at the high concentrations could possibly be attributed to aggregation due to the lower pH status at higher concentrations. In our study, a 2-fold increase in hALA concentrations showed the opposite effect with a granular pattern at the lower concentrations as opposed to a diffuse fluorescence for the higher concentrations.

The diametrically opposed response obtained with in vivo bladder PDT in rats with 2 different hALA concentrations can thus probably be attributed to the different subcellular localization of the photosensitizer PpIX. In the future, we hope to be able to more specifically define the exact subcellular sites with immunohistochemical studies. If the mitochondrial localization is confirmed in case of a granular distribution pattern, this model could be

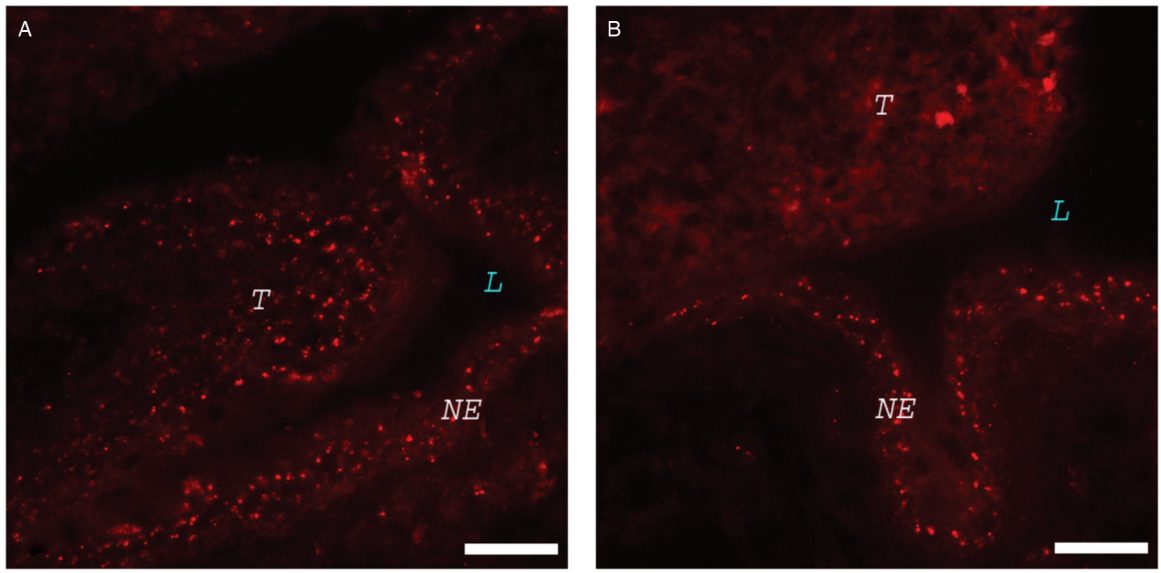

Figure 7. Confocal fluorescent microscopy obtained from tumor-bearing rat bladders sensitized with 8 (A) or 16 (B) mM hALA, respectively, showing epithelial distribution in normal and tumor epithelium within the same bladder. L = lumen; T = tumor; NE = normal epithelium; Bar = 50 μm.

extremely interesting for in vivo studies concerning apoptosis and necrosis. An hALA instillation with 16 mM in a single animal tumor-bearing bladder would then result in a mitochondrial photosensitizer localization in the nontransformed epithelium but not in the adjacent bladder tumors. A whole bladder treatment, indifferent to the subcellular localization, could thus potentially have totally different results in terms of modality of cell death and could thus be monitored in vivo or ex vivo.

Acknowledgments

The author acknowledges the technical assistance provided by the Lebanese International University that helped the completion of this work.

Statement of ethics

All applicable international, national, and/or institutional guidelines for the care and use of animals were followed.

Conflict of interest statement

No conflict of interest has been declared by the author.

Funding source

This research received no specific grant from any funding agency in the public, commercial, or not-for-profit sectors.

Author contributions

The author confirms sole responsibility for the following: study conception and design, data collection, analysis and interpretation of results, and manuscript preparation.

References

[1] Dougherty TJ. Photodynamic therapy. *Clin Chest Med* 1985;6(2):219–236.

[2] Kennedy JC, Marcus SL, Pottier RH. Photodynamic therapy (PDT) and photodiagnosis (PD) using endogenous photosensitization induced by 5-aminolevulinic acid (ALA): mechanisms and clinical results. *J Clin Laser Med Surg* 1996;14(5):289–304.

[3] Iinuma S, Farshi SS, Ortel B, Hasan T. A mechanistic study of cellular photodestruction with 5-aminolaevulinic acid-induced porphyrin. *Br J Cancer* 1994;70(1):21–28.

[4] Thunell S. Porphyrins, porphyrin metabolism and porphyrias. I. Update. *Scand J Clin Lab Invest* 2000;60(7):509–540.

[5] Sandberg S, Romslo I, Hovding G, Bjorndal T. Porphyrin-induced photodamage as related to the subcellular localization of the porphyrins. *Acta Derm Venereol Suppl (Stockh)* 1982;100(6):75–80.

[6] Wilson BC, Olivo M, Singh G. Subcellular localization of Photofrin and aminolevulinic acid and photodynamic cross-resistance in vitro in radiation-induced fibrosarcoma cells sensitive or resistant to photofrin-mediated photodynamic therapy. *Photochem Photobiol* 1997;65(1):166–176.

[7] Cox GS, Krieg M, Whitten DG. Photochemical reactivity in organized assemblies. 30. Self-sensitized photooxidation of protoporphyrin IX derivatives in aqueous surfactant solutions; product and mechanistic studies. *J Am Chem Soc* 1982;104(25):6930–6937.

[8] Moan J, Streckyte G, Bagdonas S, Bech O, Berg K. Photobleaching of protoporphyrin IX in cells incubated with 5-aminolevulinic acid. *Int J Cancer* 1997;70(1):90–97.

[9] Marti A, Lange N, van den Bergh H, Sedmera D, Jichlinski P, Kucera P. Optimisation of the formation and distribution of protoporphyrin IX in the urothelium: an in vitro approach. *J Urol* 1999;162(2):546–552.

[10] Robinson DJ, de Bruijn HS, van der Veen N, Stringer MR, Brown SB, Star WM. Fluorescence photobleaching of ALA-induced protoporphyrin IX during photodynamic therapy of normal hairless mouse skin: the effect of light dose and irradiance and the resulting biological effect. *Photochem Photobiol* 1998;67(1):140–149.

[11] van der Veen , de Bruijn HS, Star WM. Photobleaching during and re-appearance after photodynamic therapy of topical ALA-induced fluorescence in UVB-treated mouse skin. *Int J Cancer* 1997;72(1):110–118.

[12] Jichlinski P, Guillou L, Karlsen SJ, et al. Hexyl aminolevulinate fluorescence cystoscopy: a new diagnostic tool for photodiagnosis of superficial bladder cancer-a multicenter study. *J Urol* 2003;170(1):226–229.

[13] Schmidbauer J, Witjes F, Schmeller N, Donat R, Susani M, Marberger M. Improved detection of urothelial carcinoma in situ with hexaminolevulinate fluorescence cystoscopy. *J Urol* 2004;171(1):135–138.

[14] Andrejevic-Blant S, Major A, Ludicke F, et al. Time-dependent hexaminolaevulinate induced protoporphyrin IX distribution after topical application in patients with cervical intraepithelial neoplasia: a fluorescence microscopy study. *Lasers Surg Med* 2004;35(4):276–283.

[15] Ludicke F, Gabrecht T, Lange N, et al. Photodynamic diagnosis of ovarian cancer using hexaminolaevulinate: a preclinical study. *Br J Cancer* 2003;88(11):1780–1784.
[16] Stenzl A, Burger M, Fradet Y, et al. Hexaminolevulinate guided fluorescence cystoscopy reduces recurrence in patients with nonmuscle invasive bladder cancer. *J Urol* 2010;184(5):1907–1913.
[17] Grossman HB, Stenzl A, Fradet Y, et al. Long-term decrease in bladder cancer recurrence with hexaminolevulinate enabled fluorescence cystoscopy. *J Urol* 2012;188(1):58–62.
[18] Gallagher KM, Gray K, Anderson CH, et al. 'Real-life experience': recurrence rate at 3 years with Hexvix® photodynamic diagnosis-assisted TURBT compared with good quality white light TURBT in new NMIBC-a prospective controlled study. *World J Urol* 2017;35(12):1871–1877.
[19] Soergel P, Loehr-Schulz R, Hillemanns M, Landwehr S, Makowski L, Hillemanns P. Effects of photodynamic therapy using topical applied hexylaminolevulinate and methylaminolevulinate upon the integrity of cervical epithelium. *Lasers Surg Med* 2010;42(9):624–630.
[20] El Khatib S, Didelon J, Leroux A, Bezdetnaya L, Notter D, D'Hallewin M. Kinetics, biodistribution and therapeutic efficacy of hexylester 5-aminolevulinate induced photodynamic therapy in an orthotopic rat bladder tumor model. *J Urol* 2004;172(5 Pt 1):2013–2017.
[21] Xiao Z, McCallum TJ, Brown KM, et al. Characterization of a novel transplantable orthotopic rat bladder transitional cell tumour model. *Br J Cancer* 1999;81(4):638–646.
[22] Lilge L, O'Carroll C, Wilson BC. A solubilization technique for photosensitizer quantification in ex vivo tissue samples. *J Photochem Photobiol B* 1997;39(3):229–235.
[23] Bezdetnaya L, Zeghari N, Belitchenko I, et al. Spectroscopic and biological testing of photobleaching of porphyrins in solutions. *Photochem Photobiol* 1996;64(2):382–386.
[24] Lange N, Jichlinski P, Zellweger M, et al. Photodetection of early human bladder cancer based on the fluorescence of 5-aminolaevulinic acid hexylester-induced protoporphyrin IX: a pilot study. *Br J Cancer* 1999;80(1-2):185–193.
[25] Rud E, Gederaas O, Høgset A, Berg K. 5-aminolevulinic acid, but not 5-aminolevulinic acid esters, is transported into adenocarcinoma cells system BETA transporters. *Photochem Photobiol* 2000;71(5):640–647.
[26] Cosserat-Gerardin I, Bezdetnaya L, Notter D, Vigneron C, Guillemin F. Biosynthesis and photodynamic efficacy of protoporphyrin IX (PpIX) generated by 5-aminolevulinic acid (ALA) or its hexylester (hALA) in rat bladder carcinoma cells. *J Photochem Photobiol B* 2000;59(1-3):72–79.
[27] Belitchenko I, Melnikova V, Bezdetnaya L, et al. Characterization of photodegradation of meta-tetra (hydroxyphenyl) chlorin (mTHPC) in solution: biological consequences in human tumor cells. *Photochem Photobiol* 1998;67(5):584–590.
[28] Lassalle HP, Bezdetnaya L, Iani V, Juzeniene A, Guillemin F, Moan J. Photodegradation and phototransformation of 5,10,15, 20-tetrakis (m-hydroxyphenyl) bacteriochlorin (m-THPBC) in solution. *Photochem Photobiol Sci* 2004;3(11-12):999–1005.
[29] Rotomskis R, Bagdonas S, Streckyte G. Spectroscopic studies of photobleaching and photoproduct formation of porphyrins used in tumour therapy. *J Photochem Photobiol B* 1996;33(1):61–67.
[30] Boere IA, Robinson DJ, de Bruijn HS, et al. Monitoring in situ dosimetry and protoporphyrin IX fluorescence photobleaching in the normal rat esophagus during 5-aminolevulinic acid photodynamic therapy. *Photochem Photobiol* 2003;78(3):271–277.
[31] Robinson DJ, de Bruijn HS, van der Veen N, Stringer MR, Brown SB, Star WM. Protoporphyrin IX fluorescence photobleaching during ALA-mediated photodynamic therapy of UVB-induced tumors in hairless mouse skin. *Photochem Photobiol* 1999;69(1):61–67.
[32] Nadeau V, O'Dwyer M, Hamdan K, Tait I, Padgett M. In vivo measurement of 5-aminolaevulinic acid-induced protoporphyrin IX photobleaching: a comparison of red and blue light of various intensities. *Photodermatol Photoimmunol Photomed* 2004;20(4):170–174.
[33] Ruck A, Hildebrandt C, Kollner T, Schneckenburger H, Steiner R. Competition between photobleaching and fluorescence increase of photosensitizing porphyrins and tetrasulphonated chloroaluminiumphthalocyanine. *J Photochem Photobiol B* 1990;5(3-4):311–319.
[34] Schneckenburger H, Ruck A, Bartos B, Steiner R. Intracellular distribution of photosensitizing porphyrins measured by video-enhanced fluorescence microscopy. *J Photochem Photobiol B* 1988;2(3):355–363.
[35] Brun A, Sandberg S. Light-induced redistribution and photobleaching of protoporphyrin in erythrocytes from patients with erythropoietic protoporphyria: an explanation of the rapid fading of fluorocytes. *J Photochem Photobiol B* 1988;2(1):33–41.
[36] Casas A, Perotti C, Saccoliti M, Sacca P, Fukuda H, Batlle AM. ALA and ALA hexyl ester in free and liposomal formulations for the photosensitisation of tumour organ cultures. *Br J Cancer* 2002;86(5):837–842.
[37] Gaullier JM, Berg K, Peng Q, et al. Use of 5-aminolevulinic acid esters to improve photodynamic therapy on cells in culture. *Cancer Res* 1997;57(8):1481–1486.
[38] Xiang W, Weingandt H, Liessmann F, et al. Photodynamic effects induced by aminolevulinic acid esters on human cervical carcinoma cells in culture. *Photochem Photobiol* 2001;74(4):617–623.
[39] D'Hallewin MA, El Khatib S, Leroux A, Bezdetnaya L, Guillemin F. Endoscopic confocal fluorescence microscopy of normal and tumor bearing rat bladder. *J Urol* 2005;174(2):736–740.
[40] Hsieh YJ, Wu CC, Chang CJ, Yu JS. Subcellular localization of Photofrin® determines the death phenotype of human epidermoid carcinoma A431 cells triggered by photodynamic therapy: when plasma membranes are the main targets. *J Cell Physiol* 2003;194(3):363–375.
[41] Krieg RC, Messmann H, Schlottmann K, et al. Intracellular localization is a cofactor for the phototoxicity of protoporphyrin IX in the gastrointestinal tract: in vitro study. *Photochem Photobiol* 2003;78(4):393–399.
[42] Krammer B, Uberriegler K. In-vitro investigation of ALA-induced protoporphyrin IX. *J Photochem Photobiol B* 1996;36(2):121–126.

How to cite this article: El Khatib S. In vivo photobleaching kinetics and epithelial biodistribution of hexylaminolevulinate-induced protoporphyrin IX in rat bladder cancer. *Curr Urol.* 2021;15(1):2–10. doi: 10.1097/CU9.0000000000000004